Korean J. Chem. Eng., **27**(4), 1328-1332 (2010)
DOI: 10.1007/s11814-010-0187-6

Hydrodynamic characteristics of cold-bed circulating fluidized beds for the methanol to olefins process

Hyun Suk Lee*, Yoong Lee, Sang-Soon Park***, Ho-Jeong Chae***, Soon-Yong Jeong***, and Dong Hyun Lee*,†**

*Department of Chemical Engineering, SungKyunKwan University, 300 Chunchun, Jangan, Suwon 440-746, Korea
**Department of Chemical Engineering, DanKook University, 126, Yongin 448-701, Korea
***Alternative Chemicals/Fuel Research Centre, Korea Research Institute of Chemical Technology, P.O. Box 107, Yuseong-gu, Daejeon 305-600, Korea
(*Received 12 July 2009 • accepted 19 November 2009*)

Abstract−The effects of the riser inlet velocity (2.2-3.9 m/s), seal-pot inlet velocity (2.4-7.1 U_{mf}), aeration flow rate (2.5×10^{-7}-3.7×10^{-6} m^3/s) in seal-pot, and solid inventory (0.15-0.2 kg) on the hydrodynamic characteristics of a 9 mm-ID×1.9 m-high cold-bed circulating fluidized bed for methanol to olefins (MTO) process were investigated. FCC (Engelhard; 82.4 μm) particles were used as bed particles. Most of the experimental flow regimes were observed in fast fluidization and pneumatic transport regimes. The axial solid holdup in a riser increased with increasing solid mass flux and solid inventory. Solid mass flux increased proportionally until reaching a maximum value and then decreased with increasing seal-pot inlet velocity. The obtained hydrodynamic characteristics in the cold-bed circulating fluidized beds were compared with previous results.

Key words: Circulating Fluidized Bed, Solid Holdup, Solid Mass Flux, Seal-pot

INTRODUCTION

Recently, due to the rapid rise of crude oil prices, the light olefin manufacturing process for petrochemical industries has received much attention. Methanol to olefins (MTO) is a process with potential for excellent economical efficiency and commercialization, but the SAPO-34 catalyst used for the process is having deactivation problems in compliance with coking. Therefore, a circulating fluidized bed (CFB) reactor is a promising piece of equipment to establish a constant catalyst activity, maintained by coke burning through the air in the MTO process [1]. CFB reactors with high gas-solid mass transfers and low-pressure drops have been utilized in numerous petrochemical industries for FCC (fluid catalytic cracking), coal combustion, and various catalytic reactions, including the MTO process [2]. CFB catalytic reactors utilize Geldart A group particles and operate at a high gas velocity and high solid circulation rate, while CFB combustors, using Geldart B group particles, operate at lower gas velocities and solid circulation rates [3]. Understanding the solids distribution and flow behavior in the CFB risers is key to the successful design and scale-up of a CFB system [4]. Many studies into all aspects of CFB hydrodynamics have been performed [5-7]. Flow regimes in gas-solid CFBs have been characterized by solid circulation rates at a given gas velocity [8]. To accurately measure the solid holdup, pressure differences have been studied using various methods, e.g., quick closing valves, γ-ray absorption, and x-ray computed tomography [9-12]. However, the design and operation of fluidized bed reactors are by no means easy tasks, particularly when the circulation of solids is involved. Therefore, CFB technology is much more complicated than the technology associated with fixed bed reactors [13].

Operating conditions of reactors can be adjusted for the desired product yield. Lower methanol partial pressure leads to higher selectivity for light olefins such as ethylene; therefore, yield advantage can be obtained by using a methanol that typically contains around 20 wt% water [1]. Bos et al. [14] developed a kinetic model for a commercial-scale MTO process in an ethylene mode using a small-pore molecular-sieve catalyst. The kinetic model has been implemented in mathematical models of various reactors for estimation of selectivity and reactor dimension. Soundararajan et al. [15] developed a simulation for the MTO process in a CFB reactor that combined Bos's [14] model with another kinetic model for the process about the shape selectivity catalyst of SAPO-34 and the core-annulus type hydrodynamics model. In addition, the simulation evaluated the sensitivity of the coke contents upon catalyst and geometric considerations of the CFB reactor for olefin yield. Wahabi [16] developed a kinetic and deactivation model for the MTO process using SAPO-34, and compared performance between multi-bed adiabatic reactors and fluidized bed reactors based on a production rate of 55,000 tons/year of ethylene and propylene. The fluidized bed reactor proved more favorable than multi-bed adiabatic reactors based on the amount of catalyst.

There are several simulation results for MTO processes with numerous variables. In spite of the necessity of being able to design MTO reactors to work in CFB applications, insufficient experimental data for CFB design exists in the literature. Therefore, the objective of this work is to study hydrodynamic characteristics of the MTO process in a cold-bed CFB and compare it with previous works.

EXPERIMENTAL

Experiments were carried out in a 9 mm-ID×1.9 m-high cold-bed of circulating fluidized beds. It was made of a transparent acrylic column equipped with the seal-pot as a non-mechanical valve for

†To whom correspondence should be addressed.
E-mail: dhlee@skku.edu

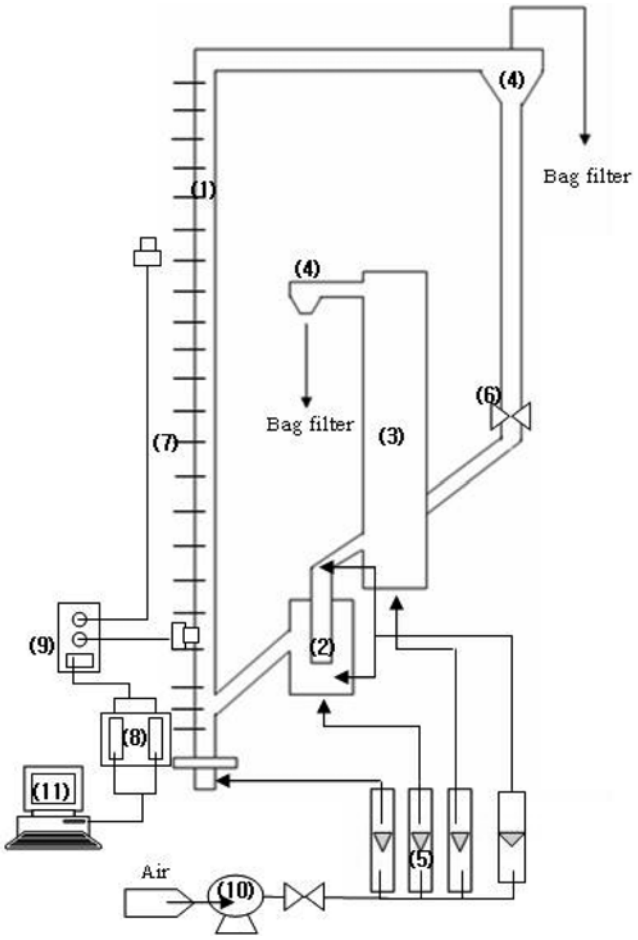

Fig. 1. Schematic diagram of cold-bed circulating fluidized bed.

1. Riser
2. Seal-pot
3. Bubbling bed
4. Cyclone
5. Air flow meter
6. Ball valve
7. Pressure tap
8. A/D converter
9. Transmitter
10. Compressor
11. PC

return of entrained particles. Fig. 1 shows the experimental apparatus consisting of a riser (9 mm-ID×1.9 m-high), bubbling bed (0.038 m-ID×0.63 m-high), and seal-pot (0.038 m-ID×0.12 m-high). For smooth, solid circulation, air was individually injected into four parts (riser, seal-pot, bubbling bed and aeration). All parts of the equipment were connected with copper lines and grounded. The pressure taps were mounted flush on the column and covered with a 250-mesh screen to prevent particles from coming in. The pressure transducer (Cole-Parmer Co., C-68071-12) was calibrated using a U-tube manometer and the pressure drops were converted into a current signal. An AD converter (COMI-ZOA, SD202) was connected to a PC employed to read the continuous pressure drop in the riser and convert current to voltage at 1 Hz for 200 s. The bubbling bed was filled with FCC (Engelhard) particles and used as bed materials. The details of the physical properties of the solid particles are summarized in Table 1. A ball valve was installed between the bottom of the cyclone and bubbling bed to measure solid mass flux of the solids circulated, at a height of accumulated particles, time period, and bulk density. To enhance the solid mass flux, an aeration tap was

Table 1. Physical properties of FCC (Engelhard)

Material	FCC (Engelhard)
d_p (μm)	82.4
ρ_s (kg/m^3)	2436
U_{mf} (mm/s)	5.0
U_b (mm/s)	15.0
U_t (m/s)	0.38
Geldart's group	A

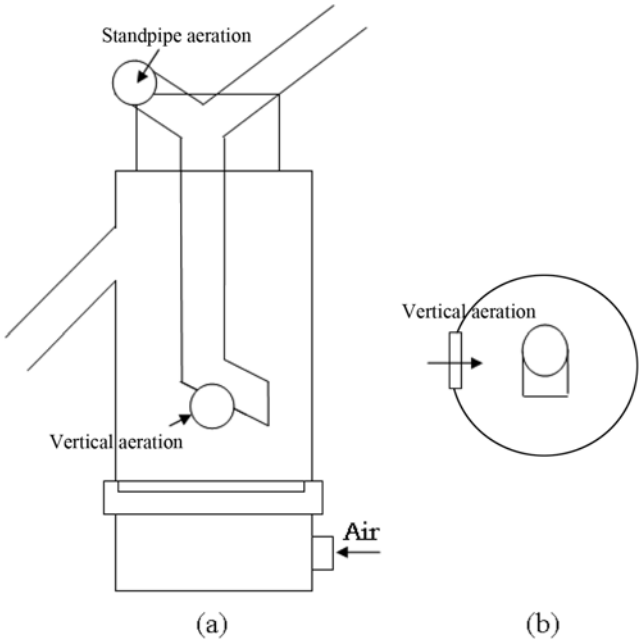

Fig. 2. Schematic diagram of seal-pot aeration part. (a) Front view of seal-pot, (b) Upper view of seal-pot.

Table 2. Experimental variables and ranges

Experimental variables	Range
U_r (m/s)	2.2-3.9
U_{seal}/U_{mf} (-)	2.4-7.1
U_A (m^3/s)	0.25-3.7×10^{-6}
Solid inventory (kg)	0.15-0.20

installed on the standpipe, and at a vertical position located 0.03 m above the perforated plate, in the seal-pot, as shown in Fig. 2.

To evaluate hydrodynamics, including solid holdup and solid mass flux, a steady state was maintained in all experiments and carried out according to Table 2.

RESULTS AND DISCUSSION

Fig. 3 shows the flow regime map for FCC particles in this study. The curve AB is a boundary line between the captive beds (bubbling beds and turbulent fluidized beds) and fast fluidization regimes. This curve was proposed by Yousfi and Gau [17] as a chocking correlation. Biswas and Leung [18] found the transition from turbulent to fast fluidization using a chocking correlation. The curve AC

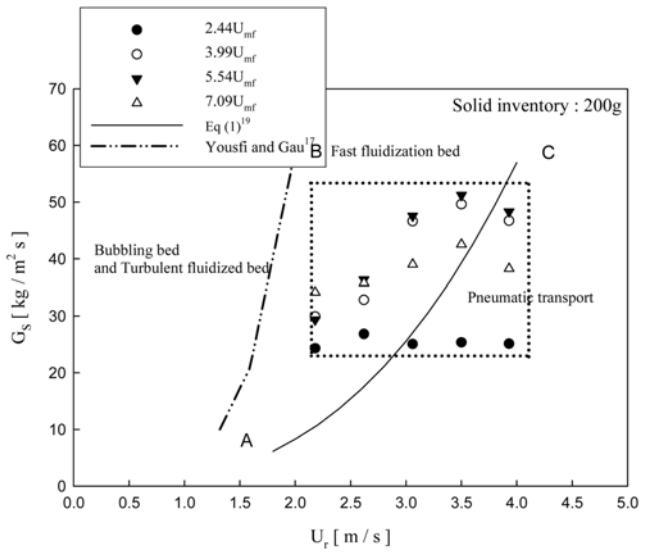

Fig. 3. Flow regime diagram for FCC particles.

is a boundary line between fast fluidization and the pneumatic transport regime. This curve is plotted by Eq. (1) presented previously in the work of Namkung et al. [19] as follows

$$\mathrm{Re}_{FD}=0.440\mathrm{Ar}^{0.563}\left(\frac{G_S}{\rho_g U_t}\right)^{0.359} \quad (1)$$

The range of variables in Eq. (1) covers $5\le \mathrm{Ar}\le 1{,}170$ and $17.0\le (G_S/\rho_S U_t)\le 1{,}040$, respectively, with a correlation coefficient of 0.991 and a standard deviation of 0.188. As shown in Fig. 3, most of the experimental regimes were observed in the regime of fast fluidization and pneumatic transport regimes.

Fig. 4 shows the variation of ε_s with the dimensionless height including data of previous works [20,21]. The axial solid holdup in the riser was determined by measuring pressure differences on riser height. The solid holdup can be expressed as follows:

$$-\frac{\Delta P}{\Delta Z}=\rho_S \varepsilon_S g \quad (2)$$

The flow at the top of a riser can be affected profoundly by the geometry of the exit port [22]. Generally, the axial solid holdup profile in a CFB riser is largely divided into two or three sections according to the exit geometry such as sharp right-angle exit or abrupt exit. In this study, the riser is divided into two sections, an acceleration zone and a fully developed zone in a riser equipped with a sharp right-angle exit. As can be seen, at a constant riser inlet velocity, solid holdup in a riser increased with increasing solid mass flux. From the sharp right-angle exit geometry in the riser chosen in this study, a fully developed region emerged over 1/2-riser height from the bottom. Any increase in curvature of the gas streamlines as the gas finds its way into the exit makes it more difficult for the particles to remain entrained and increases internal refluxing of solids in the riser [22]. The results reported by Kim [20] and Brereton [21] were different with our results at the top-section of the riser. The differences between our results and previous results [20,21] can be analyzed from the viewpoint of projected height in exit geometry. Kim et al. [23] reported that the increment of solid holdup is affected by the projected height of the exit compared with a smooth exit. Also, Grace et al. [22] concluded that the solids holdup is highest near the bottom of the riser and decreases monotonically with height right to the top when there is smooth exit or sharp right-angle exit. Therefore, the axial solids hold profile of the sharp right-angle exit made a similar trend with the smooth exit.

Fig. 5 shows the effect of ε_s with the dimensionless height on solid inventory. Axial solid holdup in the riser increased with increasing solid inventory. Riser inlet velocity was insufficient to entrain particles from seal-pot to riser as solid inventory increased; therefore, particles began to accumulate and form a dense phase at the bottom of the riser [24]. Also, these phenomena can be explained by pressure drop between bubbling bed and riser. Pressure drop between riser and bubbling bed, including the seal-pot as a non-mechanical valve, increases with increasing solid inventory in a bubbling bed. This because of the constant bubbling bed inlet gas velocity through a bubbling bed where voidage is constant and whose solid

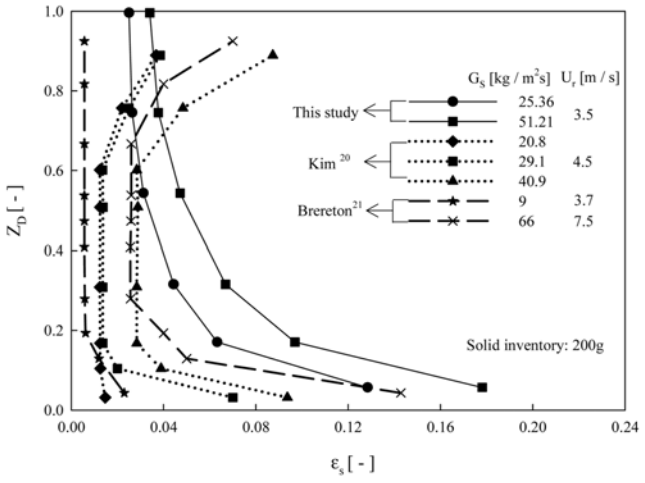

Fig. 4. Variation of the axial ε_s profile with solid circulation rate. This study: Z_t=1.95 m, Kim [20]: Z_t=7.6 m, Brereton [21]: Z_t=9.3 m.

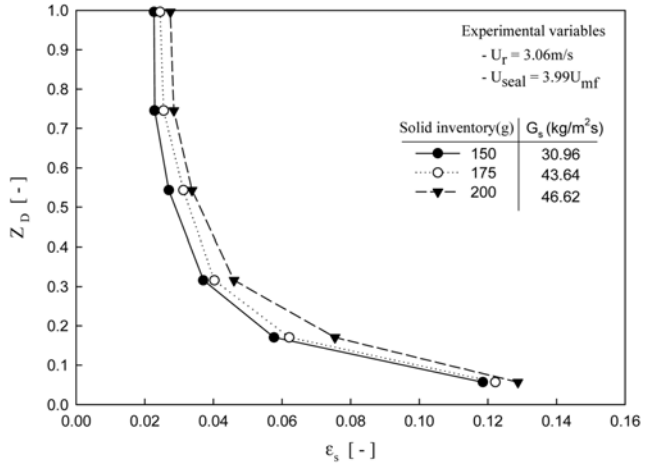

Fig. 5. Effect of the amount of solid inventory on the axial ε_s profile.

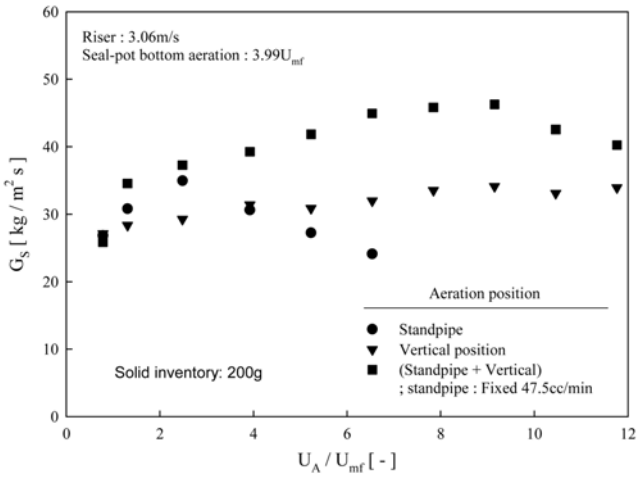

Fig. 6. Variation of solid mass flux with U_A.

height increases in proportion to the solid inventory in bubbling beds [24]. Therefore, increasing solid inventory in bubbling beds caused increasing axial solid holdup in a riser due to the increasing pressure difference between riser and bubbling beds including the seal-pot.

Fig. 6 shows the effect of the aeration flow rate (standpipe aeration, vertical position and standpipe+vertical position) on solid mass flux. As indicated, solid mass flux increased with increasing aeration flow rate in vertical aeration, but at a standpipe air injection only. Solid mass flux increased until the solid mass flux reached a maximum value ($2.5U_{mf}$) and then decreased with increasing aeration flow rate. Generally, the gas stream flowed up along the upper part of the standpipe while the particles flowed down along the bottom portion of the standpipe. However, increasing gas flow rate led to an increase in bubble frequency and coalescence. Therefore, considering the small diameter (9.0 mm) of the standpipe, bubbles at a flow rate greater than $2.5U_{mf}$ (12.4 mm/s) led to slugging. Under constant standpipe aeration (12.4 mm/s), solid mass flux was determined according to the vertical aeration. As can be seen, the solid mass flux having both sides aerated was greater than the case when only one side underwent aeration. This because the aeration flow rate in a seal-pot including the optimum standpipe aeration makes the driving force in the seal-pot to move fluidizing particles from seal-pot to riser.

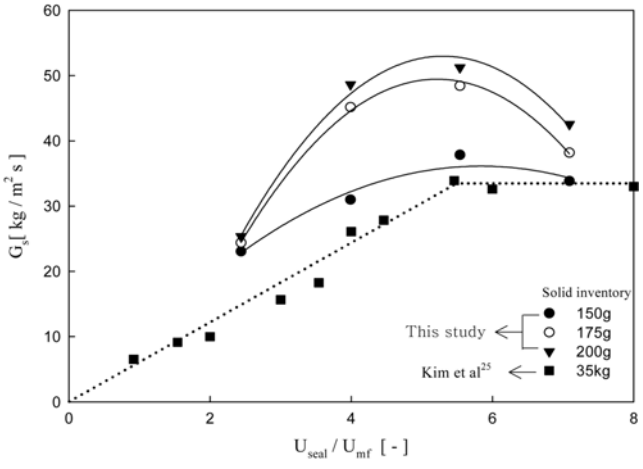

Fig. 7. Effect of seal-pot inlet velocity on solid mass flux distribution. This study: bottom aeration in seal-pot, Kim et al. [25]: vertical aeration in loop-seal.

Fig. 7 shows the effect of seal-pot inlet velocity on solid mass flux in comparison with data of a previous study [25]. As can be seen, the solid mass flux increased as the fluidizing number increased from 2.2 to $5.5U_{mf}$ in bottom aeration. Beyond $5.5U_{mf}$ it decreased slightly with increasing seal-pot inlet velocity. This result shows trends different from those of Kim et al. [25] involving FCC particles (65.0 μm) and the vertical aeration rate in a loop-seal. Considering the small dimension of the seal-pot, the solid mass flux decreased with increasing seal-pot inlet velocity due to solid irregular behavior by fluctuation beyond the maximum value.

CONCLUSION

Hydrodynamic characteristics for the MTO process were investigated in a 9 mm-ID×1.9 m-high cold-bed circulating fluidized bed reactor using air. Most of the experimental regimes were observed in fast fluidization and pneumatic transport regimes. The axial solid holdup in a riser increased with increasing solid mass flux and solid inventory. Solid mass flux through the standpipe and vertical aeration in the seal-pot was larger than aeration through only one side aeration. The solid mass flux increased proportionally until reaching a maximum value, after which it decreased as the fluidizing number in the seal-pot increased.

ACKNOWLEDGEMENTS

The authors wish to thank the Korea Ministry of Knowledge Economy (MKE) for funding through the "Project of next-generation novel technology development" of ITEP. We were partly supported by the GRRC program of Gyeonggi province through research program and instrumental support.

NOMENCLATURE

Ar : archimedes number, $d_p^3\rho_g(\rho_s-\rho_g)g/\mu^2$ [-]
d_p : mean diameter of particle [μm]
G_s : solid mass flux [kg/m^{2}s]
g : gravitational acceleration [m/s^2]
$\Delta P/\Delta Z$: differential pressure drop in a riser [N/m^3]
Re_{FD} : reynolds number of transition region between fast fluidized bed and pneumatic transport [-]
U_b : bubbling bed inlet velocity [cm/s]
U_{mf} : minimum fluidization velocity [cm/s]
U_r : riser inlet velocity [m/s]
U_{seal}/U_{mf} : seal-pot inlet velocity [-]
U_t : terminal velocity [m/s]
Z_D : dimensionless bed height in the riser [-]
Z_t : total height above the distributor in the riser [m]

Greek Symbols

ρ_g : gas density [kg/m^3]
ρ_s : particle density [kg/m^3]
ε_s : solid holdup [-]

REFERENCES

1. J. Q. Chen, A. Bozzano, B. Glover, T. Fuglerud and S. Kvisle, *Catal. Today*, **106**, 103 (2005).
2. M. Das, B. C. Meikap and R. K. Saha, *Chem. Eng. J.*, **145**, 249 (2008).
3. S. K. Gupta and F. Berruti, *Powder Technol.*, **108**, 21 (2000).
4. D. Bai and K. Kato, *Powder Technol.*, **101**, 183 (1999).
5. M. Kwauk, Fast Fluidization. Vol. 20, Advances in Chemical Engineering Series, San Diego, Academic Press (1994).
6. J. R. Grace, A. A. Avidan and T. M. Knowlton, *Circulating fluidized beds*, London, Chapman and Hall (1997).
7. F. Berruti, J. Chaouki, L. Godfroy, T. S. Pugsley and G. S. Patience, *Can. J. Chem. Eng.*, **73**, 569 (1995).
8. J. Yerushalmi and N. T. Cankurt, *Powder Technol.*, **24**, 187 (1979).
9. U. Arena, A. Cammarota and L. Pistone, *in Circulating fluidized bed technology,* P. Basu, Ed., Toronto, Pergamon Press, 119 (1986).
10. E. U. Hartge, Y. Li and J. Werther, *in Circulating fluidized bed technology*, P. Basu, Ed., Toronto, Pergamon Press, 153 (1986).
11. M. Azzi, P. Turlier and J. F. Large, *in Circulating fluidized bed technology III*, P. Basu, M. Horio and M. Hasatani, Ed., Oxford, Pergamon Press, 189 (1991).
12. T. Grassler and K. E. Wirth, *in Circulating fluidized bed technology VI*, J. Werther, Ed., Frankfurt, DECHEMA, 65 (1999).
13. G. F. Froment and K. B. Bischoff, *Chemical reactor analysis and design*, 2nd Ed., John Wiley, New York (1990).
14. A. N. R. Bos and P. J. J. Tromp, *Ind. Eng. Chem. Res.*, **34**, 3808 (1995).
15. S. Soundararajan, A. K. Dalai and F. Berruti, *Fuel*, **80**, 1187 (2001).
16. S. M. Wahabi, *Conversion of methanol to light olefins on SAPO-34 kinetic modeling and reactor design*, Ph.D. Dissertation, Texas A&M, USA (2003).
17. Y. Yousfi and G. Gau, *Chem. Eng. Sci.*, **29**, 1939 (1974).
18. J. Biswas and L. E. Leung, *Powder Technol.*, **51**, 179 (1987).
19. W. Namkung, S. W. Kim and S. D. Kim, *Chem. Eng. J.*, 7**2**, 245 (1999).
20. S. W. Kim, *Solids recycle and heat transfer characteristics in a pressurized circulating fluidized bed system*, Ph.D. Thesis, KAIST, Daejeon, Korea (2002).
21. C. M. H. Brereton, *Fluid mechanics of high velocity fluidized beds*, Ph.D. Dissertation, University of British Columbia, Vancouver, Canada (1987).
22. J. R. Grace, H. Bi and M. Golriz, *in Handbook of fluidization and fluid-particle systems*, W.-C. Yang Ed., New York, Marcel Dekker Inc. (2003).
23. S. W. Kim, S. D. Kim and D. H. Lee, *Ind. Eng. Chem. Res.*, **41**, 4949 (2002).
24. Y. J. Cho, *Hydrodynamics and heat transfer characteristics in a circulating fluidized bed*, Ph.D. Thesis, KAIST, Daejeon, Korea (1994).
25. S. W. Kim, W. Namkung and S. D. Kim, *Chem. Eng. Technol.*, **24**(8), 843 (2001).